Noise-induced pattern formation in a semiconductor nanostructure

G. Stegemann, A. G. Balanov, and E. Schöll*
Institut für Theoretische Physik, Technische Universität Berlin, D-10623 Berlin, Germany
(Received 7 September 2004; published 27 January 2005)

We investigate the influence of noise upon the dynamics of the current density distribution in a model of a semiconductor nanostructure, namely, a double barrier resonant tunneling diode. We fix the parameters of the device below the Hopf bifurcation, where the only stable state of the system is a spatially inhomogeneous "filamentary" steady state. We show that the addition of weak Gaussian white noise to the system gives rise to spatially inhomogeneous oscillations that can be quite coherent. As the noise intensity grows, the oscillations tend to become more and more spatially homogeneous, while simultaneously the temporal correlation of the oscillations decreases. Thus, while on one hand noise destroys temporal coherence, on the other hand it enhances the spatial coherence of the current density pattern.

DOI: 10.1103/PhysRevE.71.016221 PACS number(s): 05.45.−a, 05.40.−a, 72.20.Ht, 72.70.+m

I. INTRODUCTION

During recent years the double barrier resonant tunneling diode (DBRT) has become an object of great research interest [1]. It was shown that charge accumulation in such a semiconductor nanostructure provides an electrostatic feedback that, together with resonant tunneling through the energy barriers, induces strongly nonlinear Z-shaped current-voltage characteristics [2]. From a practical point of view, the latter makes the DBRT promising for applications as a key element of powerful semiconductor microwave generators. The characteristic feature of the DBRT is intrinsic bistability [2], i.e., for a range of voltages it depends upon the initial conditions whether a state of high or low current density is observed. Such a bistability creates unique conditions for a variety of interesting phenomena, including lateral spatiotemporal pattern formation of the current density [3–10]. This makes the study of the DBRT very attractive also from the viewpoint of nonlinear dynamics. While the general importance of noise is well known [11], the effects of noise upon the spatiotemporal dynamics of the current density patterns have been less studied.

In reality any process is inevitably influenced by random fluctuations. For a long time it was widely believed that the effect of noise is only destructive, smearing out any deterministic dynamics. However, recently noise has been found to evoke a very nontrivial, constructive response in nonlinear systems. It was shown, for instance, that random fluctuations are able to induce quite coherent patterns in extended media [12], to maintain existing patterns [13], and even to support wave propagation [14]. Although noise-induced phenomena were also found in semiconductor lasers [15,16], the effect of noise on charge transport in semiconductors is still an open question. The aim of the present work is to study how noise can influence current density patterns in a semiconductor nanostructure, namely, the DBRT.

The paper has the following structure. After this introduction the DBRT model and the results of our simulations are presented in Sec. II. Conclusions are drawn in Sec. III. In the Appendix some details of the model equations are given.

II. PATTERN FORMATION IN THE NOISY DBRT MODEL

Since the measurement of the local current density distribution in real devices is technically a very complicated task, the mathematical modeling still remains one of the basic methods to study pattern formation involving the charge carrier dynamics in semiconductor nanostructures. For this purpose we use a model for the DBRT suggested in [8] and add two sources of random fluctuations:

$$\frac{\partial a(x,t)}{\partial t} = f(a,u) + \frac{\partial}{\partial x}\left(D(a)\frac{\partial a}{\partial x}\right) + D_a \xi(x,t),$$

$$\varepsilon \frac{\partial u(t)}{\partial t} = U_0 - u - r\langle j\rangle + D_u \eta(t). \qquad (1)$$

All quantities in this model are dimensionless. In terms of nonlinear dynamics, this is a reaction-diffusion model of activator-inhibitor type, where a is the activator and u is the inhibitor. The dynamical variable $a(x,t)$ describes the charge carrier density inside the quantum well, which depends on time and space. The second variable $u(t)$ is the voltage drop across the device and depends only on time. The nonlinear function f models the net tunneling rate of the electrons through the two energy barriers into and out of the quantum well, and $D(a)$ is the effective diffusion coefficient, describing the diffusion of the electrons within the quantum well along the x-direction perpendicular to the current flow, $j(a,u)=\frac{1}{2}[f(a,u)+2a]$ describes the local current density in the device and $\langle j\rangle=(1/L)\int_0^L j\,dx$ gives the total current through the device. The system is assumed to satisfy Neumann boundary conditions and its width is fixed at a value of $L=30$. The first Eq. (1) is the local balance equation of the charge in the quantum well, and the second equation represents Kirchhoff's law of the circuit in which the device is operated. The external bias voltage U_0, the dimensionless load resistance r, and the time-scale ratio ε of the dynamics

*Electronic address: schoell@physik.tu-berlin.de

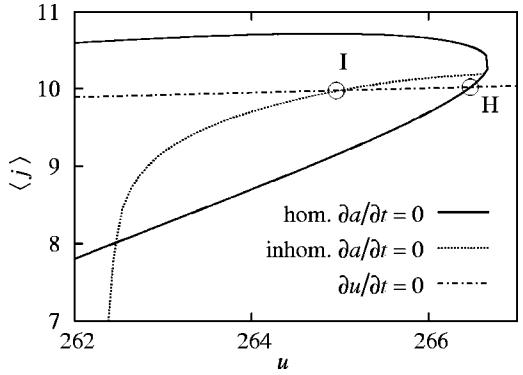

FIG. 1. Current-voltage characteristic of the DBRT model given in Eq. (1). The three lines are the null isoclines for the dynamical variables u (which is the load line, dash-dotted) and a in the case of a homogeneous $a(x)$ (solid) and in the case of inhomogeneous $a(x)$ (dotted). I and H mark the inhomogeneous and the homogeneous fixed points of the system, respectively. $U_0=-84.2895$, $r=-35$.

of u and a are parameters; ε plays the role of a bifurcation parameter which determines the stability of the fixed points in the system [10]. Physically, $\varepsilon=RC/\tau_a$ is related to the load resistance R, and the parallel capacitance C of the attached circuit, normalized by the tunneling time τ_a. The explicit form of the functions $f(a,u)$ and $D(a)$ can be found in the Appendix, and a discussion of the various deterministic bifurcation scenarios is given in [8,10].

Here we want to investigate the system under the influence of noise. For this purpose we have added the two noise terms $D_a\xi(x,t)$ and $D_u\eta(t)$, where D_a and D_u define the noise intensities in the corresponding variables and ξ and η are uncorrelated Gaussian white noise sources:

$$\langle \xi(x,t)\rangle = \langle \eta(t)\rangle = 0 \quad (x \in [0,L]),$$

$$\langle \xi(x,t)\xi(x',t')\rangle = \delta(x-x')\,\delta(t-t'),$$

$$\langle \eta(t)\,\eta(t')\rangle = \delta(t-t'). \tag{2}$$

The term $D_u\eta(t)$ represents noise in the applied voltage, whereas $D_a\xi(x,t)$ describes fluctuations of the local current density which could be caused by effective contributions, e.g., of thermal fluctuations and shot noise [17].

First consider the noise-free case $D_u=D_a=0$. For this purpose we fix $\varepsilon=6.2$ slightly below the Hopf bifurcation, which occurs at $\varepsilon\approx 6.4$. In Fig. 1 the null isoclines of the system are plotted in the current-voltage projection of the originally infinite-dimensional phase space. If the system is prepared in a completely homogeneous initial state $a(x,0)=a_0$ and no spatially inhomogeneous fluctuations are taken into account ($D_a=0$) the system (1) loses its space dependence and can be reduced to a set of two ordinary differential equations for which the null isocline $\dot{a}=0$ under this homogeneous condition can be calculated analytically from the zeros of $f(a,u)$. The intersection with the load line (null isocline $\dot{u}=0$) determines the homogeneous fixed point marked "H" in Fig. 1. Although linear stability analysis for this reduced system tells us that this is a stable focus for the parameters chosen and $\varepsilon<16.6$ with frequency $f_{\mathrm{hom}}=0.2639$ at $\varepsilon=6.2$, in the complete space-dependent system (1) this fixed point is *not* stable but still corresponds to a homogeneous steady state.

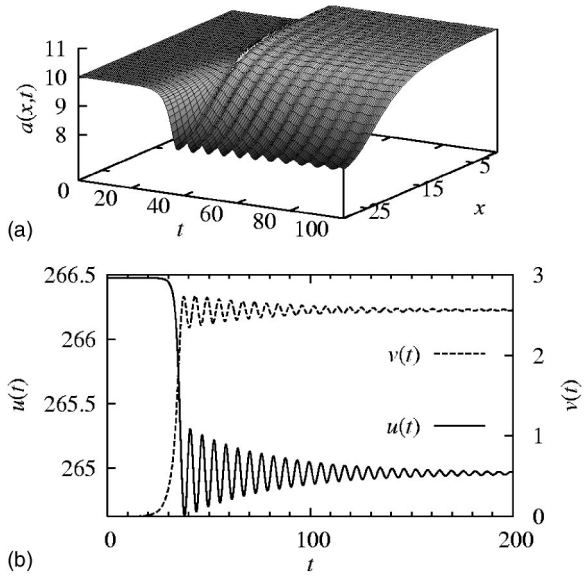

FIG. 2. Transition from the homogeneous initial state to the spatially inhomogeneous fixed point due to a small spatially inhomogeneous perturbation in the noise-free case. (a) Charge carrier density distribution $a(x,t)$. (b) Time series $v(t)$ (dashed) and $u(t)$ (solid). At $t=0$ the system is prepared in the homogeneous fixed point $u(0)=266.47$, $a(x,0)=10.02$ with a very small initial random perturbation ($D_a=0.001$). System parameters: $U_0=-84.2895$, $r=-35$, $\varepsilon=6.2$, $D_a=D_u=0$.

If we drop the condition of space independence and return to the original full system, the additional null isocline $\dot{a}=0$ with inhomogeneous $a(x,t)$ can be calculated numerically. Once again the intersection of the load line with this inhomogeneous characteristic gives a second, now inhomogeneous, fixed point ("I" in Fig. 1), which is a stable focus for $\varepsilon<6.4$. It corresponds to a current filament. If we simulate the deterministic system with ε just above the Hopf bifurcation $\varepsilon_{\mathrm{Hopf}}\approx 6.4$ of the inhomogeneous fixed point, we can determine the frequency of the limit cycle which is born out of this bifurcation as $f_{\mathrm{Hopf}}=0.1674$. Finally, the system (1) has a stable homogeneous fixed point which is characterized by negative voltage u and almost zero current density $\langle j\rangle$. This point corresponds to the nonconducting regime of the DBRT, which is beyond the scope of the present study [18]. In Fig. 2 one can see the rather rapid transition of the deterministic system from the slightly perturbed homogeneous fixed point (H) to the inhomogeneous filamentary one (I). This illustrates that for the given parameters the only stable solution, apart from a trivial, nonconducting fixed point, is an inhomogeneous steady state.

In the following we will keep the spatially inhomogeneous random perturbations of the variable a fixed at a small noise intensity of $D_a=0.001$ and investigate the behavior of the system under variation of the noise intensity D_u. Note that this noise term does not have any space-dependent influence upon a. Now we initialize the system at the inhomogeneous fixed point and simulate it with different noise in-

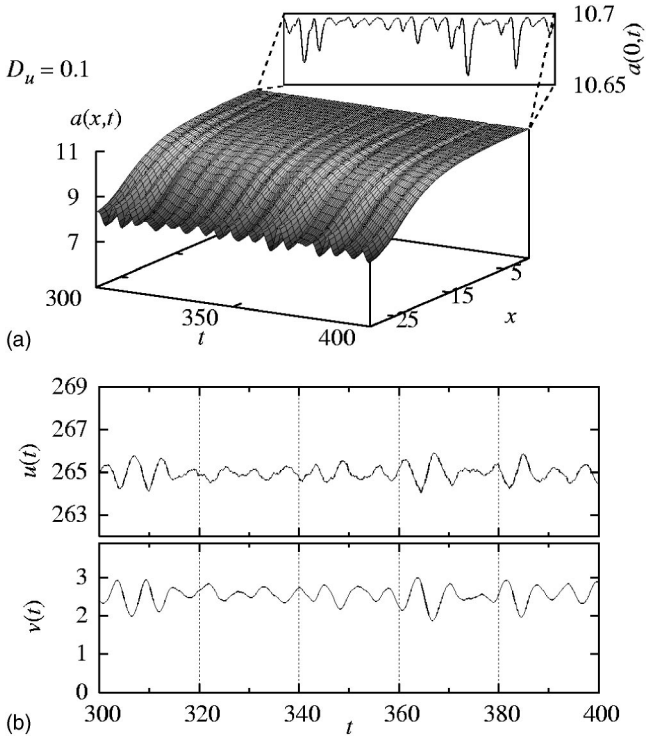

FIG. 3. Simulation of the DBRT with $D_u=0.1$, $D_a=0.001$, and initial conditions chosen at the inhomogeneous fixed point. Other parameters as in Fig. 2. Transients have been skipped. The upper panel shows the spatiotemporal dynamics of the charge carrier density with the detailed dynamics of $a(0,t)$ shown in the inset; the lower panel shows the time series of the voltage drop across the device $u(t)$ and the absolute variation $v(t)$ of the charge carrier density (for details see text).

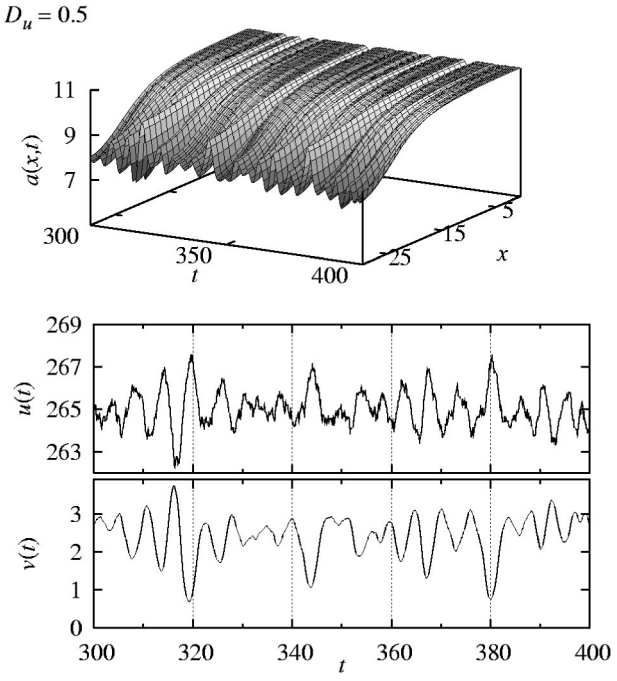

FIG. 4. Same as in Fig. 3 for $D_u=0.5$.

tensities D_u. The results can be seen in Figs. 3–5, where the upper panels illustrate the spatiotemporal dynamics and the lower panels show the oscillations of two global quantities, i.e., the voltage across the device $u(t)$ and the *absolute spatial variation* $v(t)$ of $a(x,t)$ defined by

$$v(t) \equiv \int_0^L \left| \frac{\partial a(x,t)}{\partial x} \right| dx. \tag{3}$$

While for small noise the system exhibits rather small oscillations around the inhomogeneous fixed point (Fig. 3), with increasing noise intensity a transition to completely homogeneous oscillations occurs (Fig. 5). For intermediate values of D_u one can see very nicely the competition between the inhomogeneous and the spatially homogeneous modes, the former one dominating in Fig. 4.

The behavior of $u(t)$ shows that for small noise intensity (Fig. 3) the oscillations of this variable look quite correlated, and for large noise they behave very incoherently as expected (Fig. 5). To illustrate this more clearly we calculate the Fourier power spectral densities of $u(t)$ and of $a(x,t)$, where the latter are taken at the two boundaries of the device $x=0$ and $x=L$ (Fig. 6). It is clearly seen that for small noise the spectra have very pronounced peaks [Fig. 6(a)] which indicates high correlation of the oscillations. As the noise intensity increases the spectral peaks broaden, and thus the correlation of the oscillations decreases [Figs. 6(b) and 6(c)].

As one can observe from Fig. 6(a), the power spectral density of $a(0,t)$ looks quite different from the one calculated for $a(L,t)$. In particular, while the spectra of $a(L,t)$ contain only one pronounced peak, the spectra of $a(0,t)$ include several high-order harmonics. The explanation of this fact can be obtained from Fig. 3. As one can see, while $a(L,t)$ is following the dynamics of $u(t)$, $a(0,t)$ stays fixed

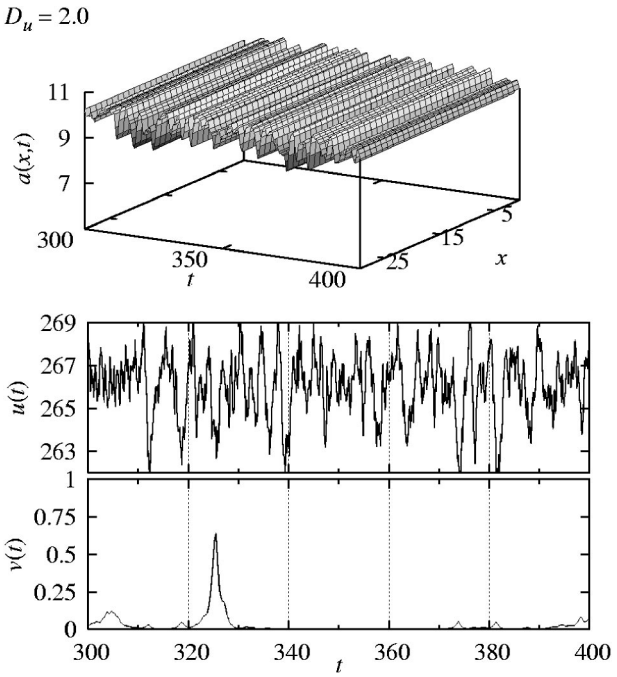

FIG. 5. Same as in Fig. 3 for $D_u=2.0$. Note the different scale for $v(t)$ at the bottom.

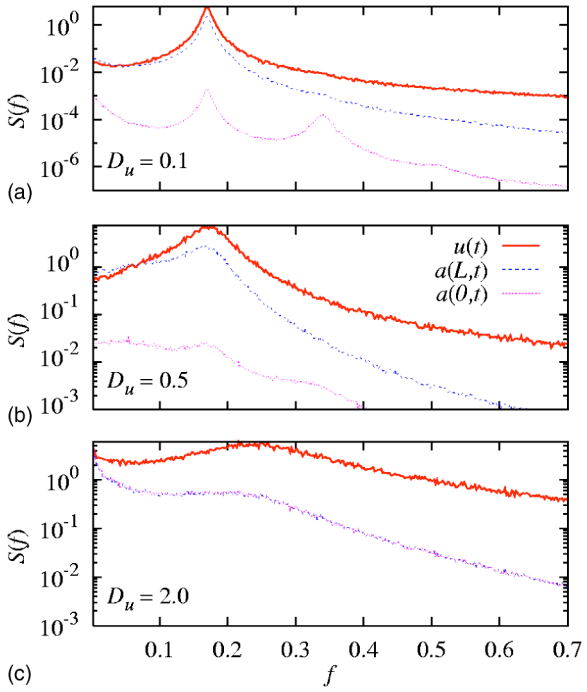

FIG. 6. (Color online) Fourier power spectral density of the dynamic variable $u(t)$ and for $a(x,t)$ at the boundaries $x=0$ and $x=L$ of the device. Parameters as in Figs. 3–5. Averages of 200 time series of length $T=2000$ have been used.

most of the time, occasionally performing spiking oscillations (small inset of Fig. 3). Such a spiking oscillation gives rise to higher harmonics in the spectra. With increasing noise intensity the difference between both boundaries of the device vanishes since the distribution of $a(x,t)$ becomes more and more homogeneous as we have seen before. In fact, in Fig. 6(c) the two corresponding curves can hardly be distinguished. We need to note that the peaks in the spectral power densities of the dynamic variable not only get smeared out with increasing noise but also shift toward higher frequencies. In Fig. 7 the position of the main peak of the power spectrum of $u(t)$ is plotted versus noise intensity D_u. While for relatively small noise strength the frequency of the noise

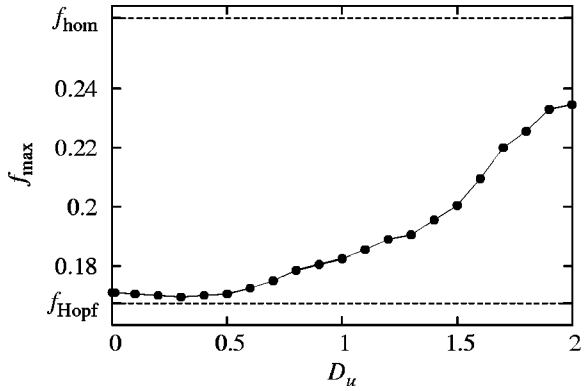

FIG. 7. Frequency shift of the noise-induced oscillations in the dependence on the noise intensity D_u. $f_{\max}$ denotes the position of the main peak of the Fourier power spectral density of $u(t)$ (cf. Fig. 6).

induced oscillation stays close to the frequency f_{Hopf} it increases with growing noise toward the frequency f_{hom} since the system gets more and more driven into the completely homogeneous state. Remember that f_{Hopf} has been defined as the frequency of the stable limit cycle, which would appear out of our inhomogeneous fixed point for $\varepsilon=\varepsilon_{\mathrm{Hopf}}$ in the deterministic system.

Let us now quantify the spatial and the temporal ordering of the system. We call the system spatially coherent if the space dependent variable $a(x,t)$ is uniformly distributed over the whole length of the device, i.e., $a(x,t)=a(t)$ for all $x \in [0,L]$ at a particular time t. This we refer to as a homogeneous state. To reveal whether a particular state of the system is spatially homogeneous or not we use, as a simple measure, the *absolute variation* $v(t)$ defined in Eq. (3) above. According to this definition a spatially homogeneous state of the system is characterized by $v(t)=0$. And the larger $v(t)$ is, the more incoherent in space (the more inhomogeneous) the system appears.

The temporal ordering of the system, on the other hand, can be measured by the correlation time [19]

$$t_{\mathrm{cor}} \equiv \frac{1}{\sigma^2}\int_0^\infty |\Psi(s)|ds, \tag{4}$$

where $\Psi(s) \equiv \langle [u(t)-\langle u\rangle][u(t+s)-\langle u\rangle]\rangle_t$ is the autocorrelation function of the variable $u(t)$ and $\sigma^2=\Psi(0)$ its variance.

By calculating the temporal mean values of $v(t)$ for different D_u we can characterize the shape of the dynamics in dependence on the noise intensity. In Fig. 8(a) these values are plotted versus the noise intensity and one can see that the mean value of v monotonically tends toward zero with increasing noise, indicating an increase in spatial coherence. The error bars in this plot show the standard deviation. In fact they reflect an essential feature of this transition, namely, the competition between spatially inhomogeneous and homogeneous modes for intermediate values of D_u. The larger the standard deviation of v is, the more "mixed" the dynamics appears. Figure 8(b) offers the same information showing the variance of v versus D_u. For noise close to zero only slight oscillations around the inhomogeneous fixed point with almost fixed spatial profile of $a(x,t)$ lead to a vanishingly small variance of v. With increasing noise, more and more frequently the system tends to a homogeneous state. The variance exhibits a maximum around $D_u=1.3$, indicating maximum fluctuations of the system between homogeneous and inhomogeneous modes. Thus, this value could be treated as a boundary between predominantly filamentary and predominantly homogeneous behavior. For even larger noise intensity the homogeneous mode is getting more and more dominant and therefore the variance of v again falls off toward zero.

On the other hand, the correlation time versus noise intensity in Fig. 8(c) shows that the temporal coherence of the system in contrast to the spatial ordering decreases rapidly with increasing noise.

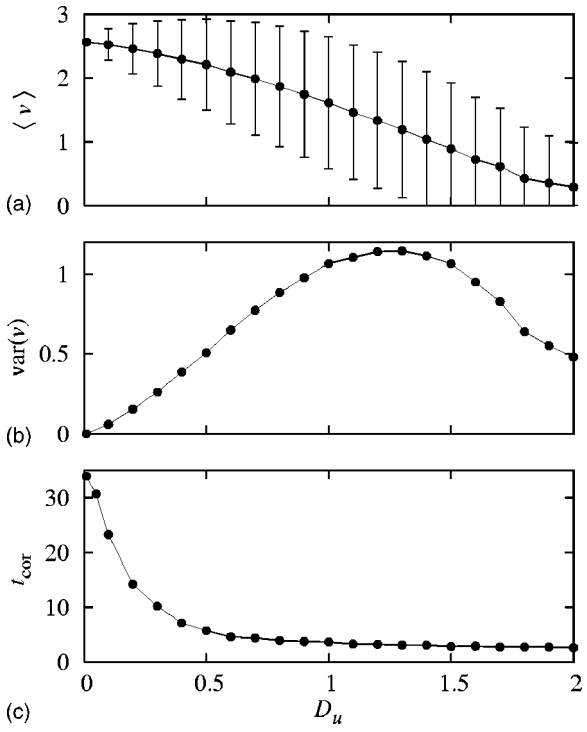

FIG. 8. Spatial and temporal ordering of the dynamics in dependence on the noise intensity D_u. (a) Time average of the order parameter $v(t)$ defined in Eq. (3); error bars correspond to the standard deviation. (b) Variance of the parameter v [corresponding to the square of the error bars from (a)]. (c) Correlation time [Eq. (4)].

III. CONCLUSION

We have investigated the complex spatiotemporal behavior of the double barrier resonant tunneling diode just below the Hopf bifurcation point under the influence of Gaussian white noise.

We have shown that random fluctuations are able to induce quite coherent oscillations of the current density in a regime where the deterministic system exhibits a stable fixed point. This extends the phenomena of noise-induced oscillations from purely time-dependent generic models, e.g., [20], to space-time patterns. Moreover, we have shown that the noise that is applied globally to a space-independent variable determines the type of spatiotemporal pattern of these oscillations. While for small noise intensity the system demonstrates oscillations which are quite correlated in time, but spatially inhomogeneous, with increasing noise intensity the shape of the spatiotemporal pattern changes qualitatively until the system reaches a highly homogeneous state. With this, the increase of spatial coherence is accompanied by the decrease of temporal correlation of the observed oscillations. In between these two situations for intermediate noise strength one can observe complex spatiotemporal behavior resulting from the competition between homogeneous and inhomogeneous oscillations.

Finally, we have examined the Fourier power spectral density of the dynamical variables and shown that with growing noise the main frequency of the oscillations shifts from the Hopf frequency of the deterministically stable inhomogeneous fixed point toward the frequency of the homogeneous fixed point. Hence we can conclude that to some extent noise of a certain intensity can stabilize the homogeneous state.

ACKNOWLEDGMENTS

This work was supported by DFG in the framework of Sfb 555. The authors are grateful to N. Janson and A. Amann for fruitful discussions.

APPENDIX

The dimensionless voltage variables u, U_0 are scaled into physical quantities by a factor of 0.35 mV. The electron density a is scaled by $10^{10}\,\mathrm{cm}^{-2}$, current density j by 500 A cm^{-2}, and the units of time and space correspond to 3.3 ps and 100 nm for typical device parameters at 4 K [8].

The effective diffusion coefficient $D(a)$ results from the inhomogeneous lateral redistribution of carriers and from the change in the local potential due to the charge accumulated in the quantum well by Poisson's equation [21]:

$$D(a) = a\left(\frac{d}{r_\mathrm{B}} + \frac{1}{1-\exp(-a)}\right), \tag{A1}$$

where $r_\mathrm{B}=(4\pi\epsilon\epsilon_0\hbar^2)/(e^2m)$ is the effective Bohr radius in the semiconductor material, ϵ and ϵ_0 are the relative and absolute permittivity of the material, and d is the effective thickness of the double barrier structure.

The function f is obtained from microscopic consideration of the tunneling currents from the emitter into the quantum well and from there to the emitter [8]:

$$f(a,u) = \left\{\frac{1}{2} + \frac{1}{\pi}\arctan\left[\frac{2}{\gamma}\left(x_0 - \frac{u}{2} + \frac{d}{r_\mathrm{B}}a\right)\right]\right\} \times\left\{\ln\left[1+\exp\left(\eta_e - x_0 + \frac{u}{2} - \frac{d}{r_\mathrm{B}}a\right)\right] - a\right\} - a. \tag{A2}$$

x_0 and γ describe the energy level and the broadening of the electron states in the quantum well and η_e is the dimensionless Fermi level in the emitter, all in units of $k_\mathrm{B}T$. Throughout the paper we use values of $\gamma=6$, $d/r_\mathrm{B}=2$, $\eta_e=28$, and $x_0=114$.

[1] E. Schöll, *Nonlinear Spatio-Temporal Dynamics and Chaos in Semiconductors* (Cambridge University Press, Cambridge, UK, 2001).
[2] V. J. Goldman, D. C. Tsui, and J. E. Cunningham, Phys. Rev. Lett. **58**, 1256 (1987).
[3] A. Wacker and E. Schöll, J. Appl. Phys. **78**, 7352 (1995).
[4] B. A. Glavin, V. A. Kochelap, and V. V. Mitin, Phys. Rev. B **56**, 13346 (1997).
[5] D. Mel'nikov and A. Podlivaev, Semiconductors **32**, 206 (1998).
[6] M. N. Feiginov and V. A. Volkov, JETP Lett. **68**, 662 (1998).
[7] M. Meixner, P. Rodin, E. Schöll, and A. Wacker, Eur. Phys. J. B **13**, 157 (2000).
[8] E. Schöll, A. Amann, M. Rudolf, and J. Unkelbach, Physica B **314**, 113 (2002).
[9] P. Rodin and E. Schöll, J. Appl. Phys. **93**, 6347 (2003).
[10] J. Unkelbach, A. Amann, W. Just, and E. Schöll, Phys. Rev. E **68**, 026204 (2003).
[11] Y. M. Blanter and M. Büttiker, Phys. Rep. **336**, 1 (2000).
[12] J. García-Ojalvo, A. Hernández-Machado, and J. M. Sancho, Phys. Rev. Lett. **71**, 1542 (1993).
[13] S. Alonso, I. Sendiña-Nadal, V. Pérez-Muñuzuri, J. M. Sancho, and F. Sagués, Phys. Rev. Lett. **87**, 078302 (2001).
[14] S. Kádár, J. Wang, and K. Showalter, Nature (London) **391**, 770 (1998).
[15] G. Giacomelli, M. Giudici, S. Balle, and J. R. Tredicce, Phys. Rev. Lett. **84**, 3298 (2000).
[16] V. V. Sherstnev, A. Krier, A. G. Balanov, N. B. Janson, A. N. Silchenko, and P. V. E. McClintock, Fluct. Noise Lett. **1**, 91 (2003).
[17] L. L. Bonilla, O. Sánchez, and J. Soler, Phys. Rev. B **65**, 195308 (2002).
[18] Although the existence of this stable point can in principle influence the dynamics of the system forced by Gaussian white noise, in fact, we can ignore it. As our study shows, for given initial conditions and the range of noise intensities that we operate with, the trajectory does not come close to the vicinity of the nonconducting fixed point for reasonably long times (of the order of 10^6 time units).
[19] R. L. Stratonovich, *Topics in the Theory of Random Noise* (Gordon and Breach, New York, 1963), Vol. 1.
[20] N. B. Janson, A. G. Balanov, and E. Schöll, Phys. Rev. Lett. **93**, 010601 (2004).
[21] V. Cheianov, P. Rodin, and E. Schöll, Phys. Rev. B **62**, 9966 (2000).